

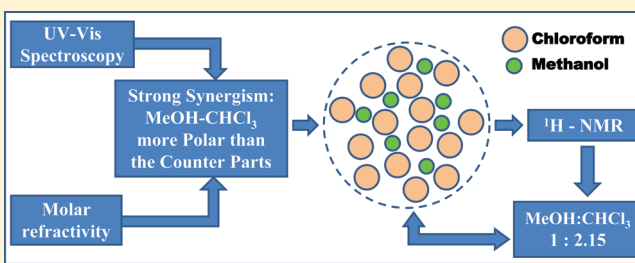
Origin of Strong Synergism in Weakly Perturbed Binary Solvent System: A Case Study of Primary Alcohols and Chlorinated Methanes

Shradhey Gupta, Shahnawaz Rafiq, Mainak Kundu, and Pratik Sen*

Department of Chemistry, Indian Institute of Technology Kanpur, Kanpur, UP, PIN-208 016, India

 Supporting Information

ABSTRACT: A strong synergistic solvation was observed for the mixtures of hydrogen bond donating and accepting solvent pairs. The nature of the interactions between two solvent pairs was investigated with different dye molecules viz. coumarin 480, coumarin 153, 4-aminophthalimide, and *p*-nitroaniline. Coumarin 480 in different alcohol–CHCl₃ (alcohols: MeOH, EtOH, BuOH) binary mixture shows a strong synergism, which is explained in the backdrop of solvent–solvent interactions. Fluorescence quenching of C480 by 1,2-phenylenediamine in the binary solvent mixture exhibited the maximum deviation in quenching constant corresponding to ~0.45 mol fraction of MeOH in MeOH–CHCl₃ binary mixture and hence suggested the maximum extent of hydrogen-bonding interactions prevailing at this proportion of mixture. The solvation behavior of MeOH–CHCl₃ mixture shows strong probe dependence with no synergism observed in *p*-nitroaniline, which is ascribed to its higher ground state dipole moment (8.8 D) relative to C480 (6.3 D). Interestingly, the strong synergistic signature observed through spectrophotometric measurement of C480 in alcohol–CHCl₃ binary mixture is absent when studied by fluorescence measurement. The higher excited state dipole moment of coumarin 480 (13.1 D) is considered to be the driving force for the absence of synergism in the excited state. In such strongly perturbed systems (due to high dipole moment values) the dominant phenomenon is preferential solvation. Analysis of proton NMR of MeOH–CHCl₃ binary solvent mixture indicates the existence of MeOH–CHCl₃ clusters in the stoichiometric ratio of 1:2.15. Refractive index measurement also infers the existence of hydrogen bonded network structure between MeOH and CHCl₃. A modified Bosch solvent exchange model has been used to determine the feasibility of synergistic behavior and polarity parameter of the mixed solvent structure of MeOH–CHCl₃ binary solvent mixture.



1. INTRODUCTION

The spectroscopic studies of molecules and clusters have crossed the boundaries of homogeneous medium and a lot of concern is being devoted to understand the behavior in micro heterogeneous systems.^{1–3} Recently, solvent mixtures made attract a lot of attention because of its unique behavior compared to its constituent counterpart and explained in terms of differential interaction leading to the formation of micro heterogeneous environment.^{3–11} The use of solvent mixtures provide the means of modification of solute–solvent interactions by virtue of its composition. The solute–solvent interaction is generally monitored in terms of the stabilization of its electronic energy level and this interaction depends on the proportion of either of the constituting solvents and is known for several years.^{12–17} The behavior of molecules in binary solvent mixture depends on either one or both solvent component by specific interactions, e.g., hydrogen bonding, self-association or by nonspecific interactions such as dipole–dipole, dipole–induced dipole interactions.^{3,11–16} In binary solvent mixtures, the deviation from ideality is believed to originate from the nature and extent of solute–solvent interactions, locally developed in the immediate vicinity of the solute molecules, which has an impact on the spectroscopic properties of the molecules. Generally, solvent

polarizability, H-bond donating ability (HBD) and H-bond accepting ability (HBA) or solvent basicity are three parameters which have been characterized to represent the variation of solute–solvent interactions.^{18,19} All these parameters are solvatochromic parameter (represented like as π^* , α , and β respectively, the Kamlet–Taft parameters) and provide information about the different mode of solvent interaction with the probe molecules in pure solvents and also in solvent mixtures.^{18–25} Characterization of solvation behavior has been done employing various methods like conductance or transfer measurements,²⁶ NMR chemical shifts,^{27–30} vibrational spectroscopy,^{3,11} UV–vis spectroscopy,^{14–17} solvation dynamics,^{1,7} etc. Refractive index measurements of binary solvent mixtures have also been to determine the quantitative information about the solvent–solvent interactions.^{31,32}

In solvent mixtures the proportion of constituting solvents may substantially differ around the solute compared to that in bulk resulting the change in Gibbs energy of solvation. This would be the resultant of probe being solvated preferentially by

Received: August 12, 2011

Revised: December 23, 2011

Published: December 26, 2011

one of the solvents in the mixture.^{6,34} The phenomenon, where one solvent solvates the solute predominantly than the other, through specific or nonspecific solute–solvent interactions, is known as “preferential solvation”. It has been studied both experimentally,^{13–17,23–25,35–37} and theoretically^{12,33,38–40} to a great deal. Apart from preferential solvation, there is always some probability where both the constituent solvents can solvate the molecules together by mutual interaction and giving rise to a completely different solvation environment. Such a phenomenon is observed for some specific solvent pairs and is termed as “Synergism”.²⁰ In synergism, the solvent mixture constituting the solvation shell around the probe acts as a completely different entity and behaves distinctly than either of the bulk solvents. In general, synergism is the significant change of a particular property (e.g., solvation in the present case) from its bulk counterparts. Mancini et al.²⁰ proposed that the combination of dipolarity and hydrogen bond donating and accepting capacity of solvents leads synergistic effect in binary solvent mixtures, which is clearly reflected through $E_T(30)$ empirical solvent polarity parameter. They measured the kinetics of 1-fluoro-2,4-nitrobenzene with morpholine and piperidine in several binary mixtures of polar aprotic H-bond accepting solvents like acetonitrile and chloroform and observed that the binary solvent mixture exhibited synergism. Kessler et al.⁴¹ on the basis of molecular dynamic simulations revealed clustering effect in the MeOH–CHCl₃ solvent mixture. They also demonstrated that such a mixture preferentially solvates the hydrophilic and hydrophobic parts of amphiphilic solutes. Durov et al.⁴² calculated the excess thermodynamic functions and dielectric permittivity of MeOH–CHCl₃ mixture in the framework of quasichemical model of nonideal association solution and reproduced the physicochemical properties of the mixture to a good accuracy. This model, based on supramolecular aggregate formation, proposing that deviation from ideality is predominantly due to parallel orientation of dipoles in the methanol aggregates and in the complexes with chloroform. The deviations from ideality can also be explained in terms of the heterogeneity at a microscopic level^{41,42} and the self-association of alcohol molecules.⁴³ This homonuclear or heteronuclear clustering of molecules has been attributed to large negative excess entropy of MeOH–CHCl₃ mixture.³⁴ Recently Bhattacharyya et al.⁴⁴ measured the thermal-lens signals as a function of relative proportion of binary solvent mixtures and proposed it dependence on the extent of interaction between the molecules of the solvent mixture.

In spite of the large number of studies, the experimental determination of the nature of solvation cage in the binary solvent mixture has not yet been well established. In the present contribution, we throw light on the origin of synergism in MeOH–CHCl₃ binary solvent mixture using electronic spectroscopy, refractive index measurements, proton NMR measurements, fluorescence quenching study, and solvent exchange model. The probe dependence behavior of the solvation shell was also studied, and its impact was discussed.

2. EXPERIMENTAL SECTION

2.1. Materials. Coumarin 480 (C480), Coumarin 153 (C153), and 1,2-phenylenediamine (PDA) were purchased from Sigma-Aldrich Chemical Company, USA, and used without further purification. 4-Aminophthalimide (4-AP, Kodak) was purified by repeated recrystallization from a methanol–water mixture. *p*-nitroaniline (*p*NA) was purchased from Avra Chemical Company,

India, and was recrystallized from ethanol, vacuum-dried and confirmed by NMR before used. High performance liquid chromatography (HPLC) grade methanol, chloroform, *n*-butanol were purchased from Merck, India. Carbon tetrachloride was purchased from RFCL Ltd., India. Ethanol was purchased from Les Alcools, Canada. The experiments have been done with the solvents after proper treatment to remove moisture. Everytime we have done the experiment with freshly distilled solvents to avoid any moisture contamination. Care was also taken to avoid contamination by moisture during the sample preparation and experiments. All the measurements have been done at 25 °C.

2.2. Methods. The UV–visible absorption spectra and fluorescence spectra of the sample solutions were measured by a commercial UV–visible spectrophotometer (UV-2401, Shimadzu) and fluorimeter (Spex, Fluoromax-4, Jobin-Yvon) respectively. Fluorescence lifetime was measured by single photon counting method using a commercial setup from Jobin-Yvon. For lifetime measurement, all the samples were excited at 340 nm using a nano-LED. Abbe's refractometer (Metz-1408, Metzer Optical Instruments, India) was used to measure the refractive indices of the sample solutions.¹H NMR spectra of the samples were measured by commercial spectrometer (JEOL ECX-500, Japan) operating at 500 MHz. Tetramethylsilane was used as reference.

3. RESULTS AND DISCUSSION

3.1. Absorption and Emission Study in Different Binary Solvent Mixtures. The absorption spectra of organic dyes viz. Coumarin 480 (C480), Coumarin 153 (C153), 4-aminophthalimide (4-AP), and *p*-nitroaniline (*p*NA) were measured in several binary solvent mixtures of different compositions. In the present work, we studied different binary solvent mixture of alcohols and chlorinated methanes (alcohol = methanol, ethanol, *n*-butanol; chlorinated methane = chloroform, carbon tetrachloride). The concentration of dyes was maintained at 10^{−5} M to suffice very negligible solute–solute interactions such that intersolute effect makes no significant contribution to the solvent–solvent interactions. In order to portray the stability of different dyes in the corresponding binary mixtures, we invoke the concept of molar electronic transition energy, E_T (kcal mol^{−1}) whose relationship with absorption maximum (λ_{\max}) is given as^{45,46}

$$E_T = 28591/\lambda_{\max} \text{ (nm)} \quad (1)$$

In an ideal case, where all solvent–solvent interactions are considered to be equal, the dyes are characterized by maximum value of molar electronic transition energy given by^{10,17}

$$E_T(\text{ideal}) = X_{S1}E_{T(S1)} + X_{S2}E_{T(S2)} \quad (2)$$

where X_{S1} and X_{S2} are mole fractions of solvent 1 and solvent 2 respectively and $E_{T(S1)}$ and $E_{T(S2)}$ are E_T values of a dye or indicator solute in pure solvents 1 and 2. From this equation, it follows that in an ideal binary solvent mixture, the variation of E_T as a function of mole fraction of any component should always be linear. However generally the variation is not linear, which points toward the existence of some specific/nonspecific interactions between the dye molecule and one of the components of the mixture, which is known as preferential solvation. Apart from this, the deviation from the ideal behavior may also arise from the interaction between the solvent counterparts in the binary solvent mixture, showing a synergistic effect.

The absorption spectra of C480 in MeOH, CCl₄, and various proportions of MeOH–CCl₄ binary mixtures are shown in

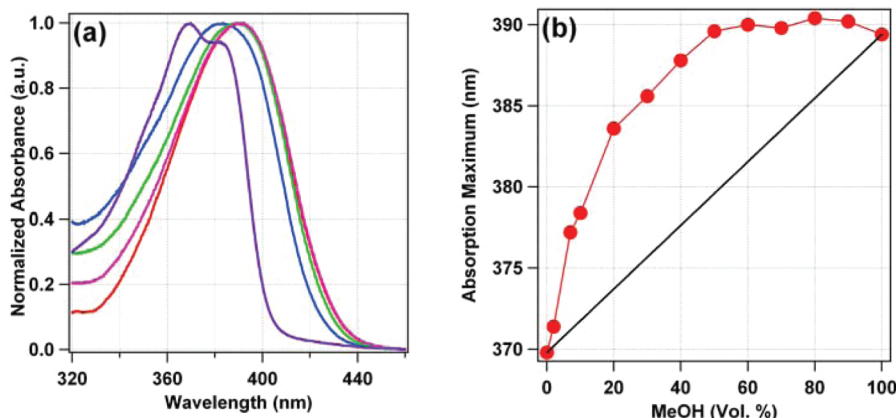


Figure 1. (a) Normalized steady state absorption spectra of C480 in bulk carbon tetrachloride, bulk methanol, 20%, 50%, and 80% MeOH–CCl₄ binary solvent mixture. The respective absorption maxima are 369.8, 390.2, 383.6, 389.6, and 390.4 nm. (b) Absorption maxima of C480 plotted against volume fraction of MeOH in MeOH–CCl₄ binary mixture.

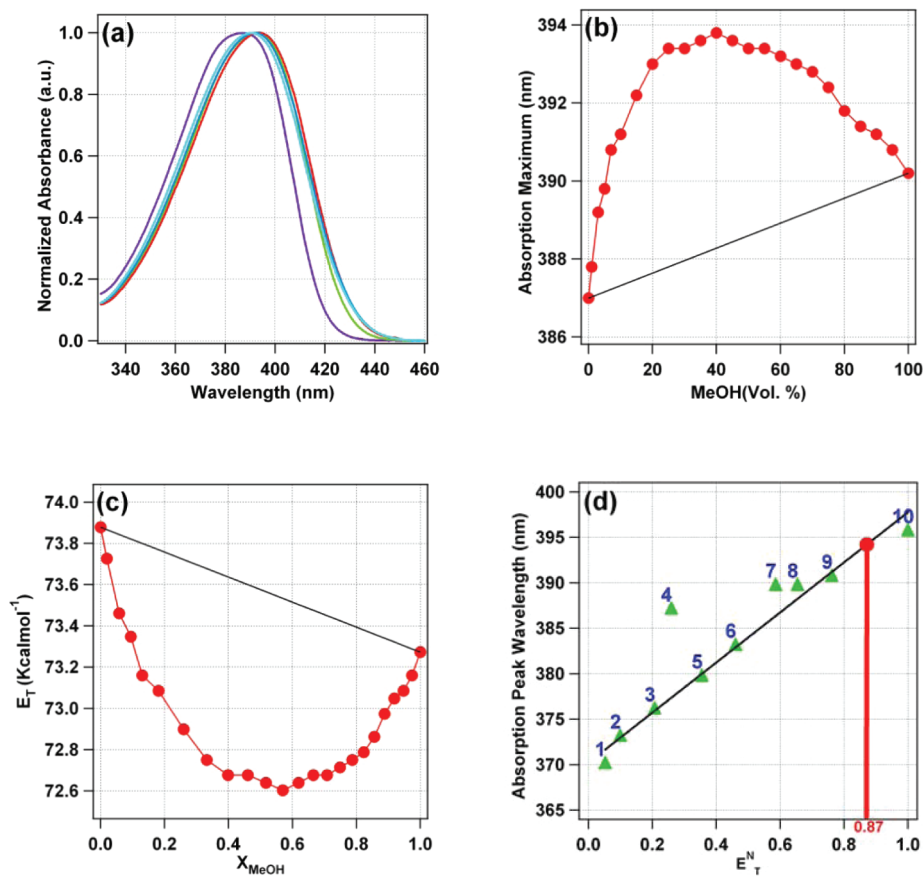


Figure 2. (a) Normalized steady state absorption spectra of C480 in bulk chloroform, bulk methanol, 20%, 50%, and 80% MeOH–CHCl₃ binary solvent mixture. The respective absorption maxima are 387, 390.2, 393, 394.4, and 391.8 nm. (b) Absorption maxima of C480 plotted against volume fraction of MeOH in MeOH–CHCl₃ binary mixture. (c) Molar transition energy of C480 plotted as a function of MeOH mole fraction in MeOH–CHCl₃ binary mixture. (d) Plot of absorption maxima of coumarin 480 in 10 solvents against the solvent E_T^N values (green ▲). The solvents plotted are carbon tetrachloride (1), toluene (2), THF (3), CHCl₃ (4), acetone (5), ACN (6), *n*-butanol (7), ethanol (8), methanol (9), and water (10). Solid black line represents the best fit of the data. The absorption maximum of C480 in 0.46 mol fraction of MeOH in MeOH–CHCl₃ binary mixture is appended on the best fit line designated by a solid red circle. The vertical red line shows the corresponding E_T^N value experienced by C480 in the 0.46 mol fraction of MeOH in the MeOH–CHCl₃ binary mixture.

Figure 1a. C480 is characterized by an absorption maximum of 370, 389.6, and 390.2 nm in pure CCl₄, 50% (v/v) volume fraction of MeOH in MeOH–CCl₄ mixture and in pure MeOH.

The variation of absorption maxima of C480 as a function of volume fraction of methanol in MeOH–CCl₄ binary mixture is shown in Figure 1b. The plot clearly shows that, as the methanol

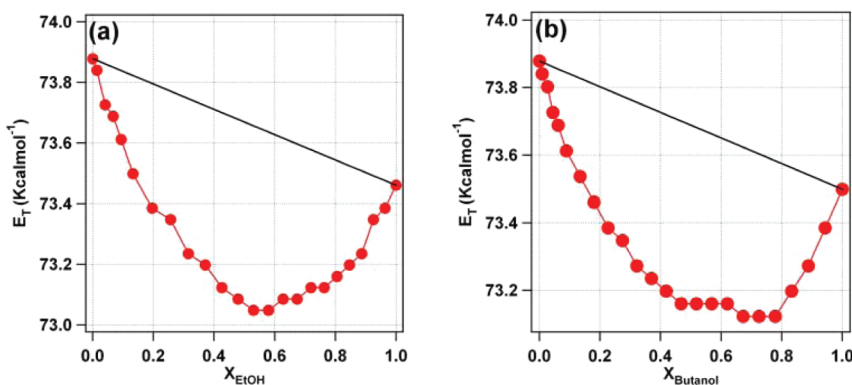


Figure 3. Molar transition energy of C480 plotted against the mole fraction of (a) ethanol in $\text{EtOH}-\text{CHCl}_3$ mixture and (b) *n*-butanol in a $n\text{-BuOH}-\text{CHCl}_3$ binary mixture. In both the graphs maximum solvatochromic stabilization to the dye in ground state is provided by binary mixture instead of either of bulk solvents and is thus a representation of synergistic solvation.

proportion is increased, the absorption maximum keeps on shifting toward the longer wavelength region. The variation of λ_{max} with MeOH volume fraction clearly suggests that MeOH molecules are solvating C480 preferentially. In this case, the absorption maxima of C480 in all the mixtures are in between the pure MeOH and CCl_4 with no signature of synergism. A similar behavior of preferential solvation is being exhibited by C480 in $\text{EtOH}-\text{CCl}_4$ and $n\text{-BuOH}-\text{CCl}_4$ binary mixtures (see Supporting Information).

However, once the CCl_4 is being replaced by CHCl_3 , the variation of absorption maxima as a function of MeOH volume fraction changed unexpectedly. Figure 2a shows the absorption spectra of C480 in MeOH– CHCl_3 binary mixture for few different MeOH volume fraction (0%, 20%, 50%, 80%, 100%). The absorption maximum of C480 in pure CHCl_3 and pure MeOH are observed at 387 and 390.2 nm, respectively. In 20%, 50%, and 80% volume fraction of MeOH, the absorption maximum is found at 393, 393.4, and 391.8 nm, respectively. This clearly indicates that the MeOH– CHCl_3 mixture provides more polar environment and hence solvate C480 more efficiently compared to pure MeOH or CHCl_3 . The dependence of absorption maximum of C480 as MeOH volume fraction in MeOH– CHCl_3 binary solvent mixture is shown in Figure 2b. In terms of molar transition energy, E_T , which gives the direct measure of stabilization energy on account of solvation, the variation is shown as a function of mole fraction of MeOH in MeOH– CHCl_3 binary mixture (Figure 2c). It is observed that, maximum stabilization in terms of solvation is provided by ~ 0.45 mol fraction of MeOH after subtracting the ideal behavior of the dye in the binary mixture according to eq 2 (see Supporting Information). The efficient solvation carried out by mixed solvent inferences toward the prevalence of mutual solvation around the solvatochromic probe molecule and such a phenomenon is called synergism. This suggests that the binary mixture acts as a different entity than either of the bulk solvents, and its mutual interaction seems to be stronger than the pure bulk solvents. Similar kind of observation was found for C480 in $\text{EtOH}-\text{CHCl}_3$ and $n\text{-BuOH}-\text{CHCl}_3$ binary mixture. The dependence of molar transition energy on the mole fraction of EtOH and $n\text{-BuOH}$ in respective $\text{EtOH}-\text{CHCl}_3$ and $n\text{-BuOH}-\text{CHCl}_3$ binary mixtures are shown in Figure 3a and 3b respectively (see also Supporting Information).

In order to discuss the solvatochromic shifts observed in MeOH– CHCl_3 binary solvent mixture quantitatively, we analyzed the

data using $E_{T(30)}^N$ polarity scale with water polarity defined as unity.⁴⁵ The aim is to find the total stabilization energy gained by solute molecule from the solvation environment in the MeOH– CHCl_3 mixture with strongest interactions, which is ~ 0.45 mol fraction of MeOH. The absorption maxima of C480 obtained in ten different solvents are plotted against solvent $E_{T(30)}^N$ values. The data was best fitted by a straight line (Figure 2d). The peak position of C480 in ~ 0.45 mol fraction MeOH– CHCl_3 binary mixture was appended on the line of best linear fit and the observed $E_{T(30)}^N$ value of this binary mixture was found to be 0.87. This value quantifies the different polarity sensed by C480 in the MeOH– CHCl_3 binary mixture and also the different stabilization energy, which is higher than that in pure methanol and chloroform.

To ensure whether the type of solvation occurring in the binary system (preferential or synergistic) is purely a function of intra/inter-solvent interactions or it as well shows some dependence on the probe molecule, probe dependent spectrophotometric measurements were pursued in the MeOH– CHCl_3 binary mixtures with C153, 4-AP, and *p*NA as the corresponding probe molecules. The variation of molar transition energy of all the probe molecules mentioned above are plotted against the mole fraction of MeOH as shown in Figure 4. It is observed that, for C153 and 4-AP (like C480) the large solvatochromic stabilization is deciphered by the MeOH– CHCl_3 binary mixture instead of pure solvent counterparts. However, this is not the case with *p*NA. In *p*NA, the ground state solvatochromic stabilization offered by the binary solvent mixture does not exceed than the bulk counterpart. This intriguing result enunciates that the type of solvation not only depends on intra/inter-solvent interactions, but also on the property of the probe molecules. The plots shown in Figure 5 represent the dependence of fluorescence emission maxima of C480 and 4-AP in MeOH– CHCl_3 binary mixture of different compositions. C480 is characterized by an emission maximum of 438, 465.6, and 474 nm in bulk CHCl_3 , 50% (v/v) MeOH– CHCl_3 and bulk MeOH. For 4-AP the respective emission maximum are 465.4, 526.2, and 527.4 nm. In both the cases, it is well evident that the excited state solvatochromic stabilization provided by the binary mixture does not exceed than the bulk CHCl_3 and MeOH.

The prevalence or absence of synergism is credited to the feasibility of hydrogen bonding network formation. The components of a binary mixture which are capable of forming hydrogen bonding network with each other tend to solvate the

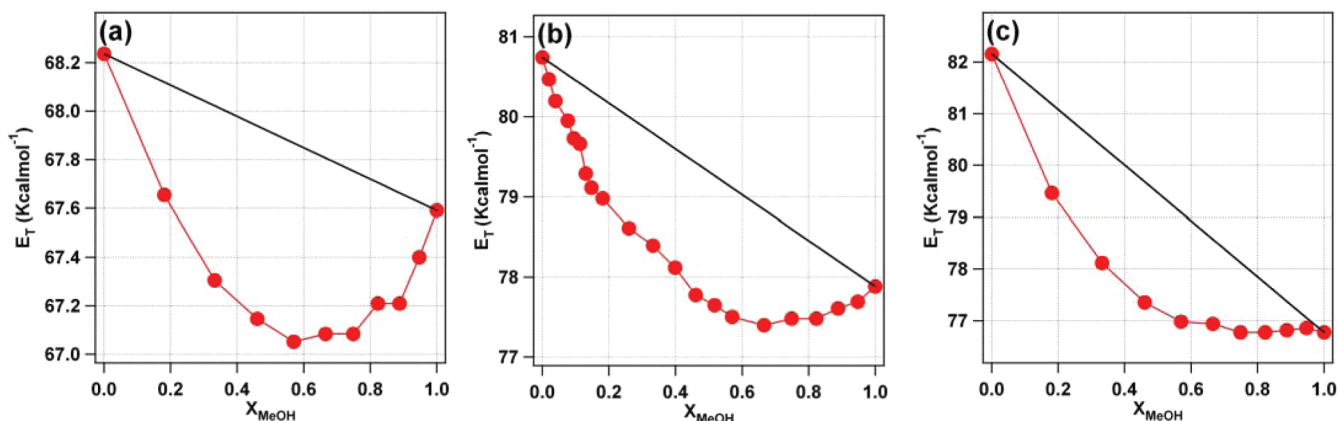


Figure 4. Molar transition energy plotted of different probe molecules; (a) C153, (b) 4-AP, and (c) *p*NA against the mole fraction of MeOH in MeOH–CHCl₃ binary mixture. In graphs a and b, maximum solvatochromic stabilization to the dye in the ground state is provided by binary mixture instead of either of bulk solvents and is thus a representation of synergistic solvation. While as in case of *p*NA, MeOH molecules are solvating the probe preferentially, as the stabilization provided by binary mixture is same as that provided by bulk methanol.

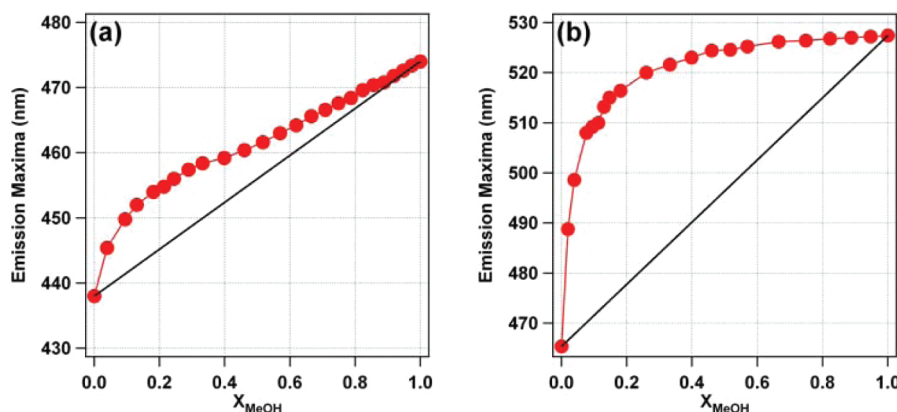


Figure 5. Emission maxima of (a) C480 and (b) 4-AP plotted against volume fraction of MeOH in MeOH–CHCl₃ binary mixture. It is clearly evident that, in both cases, the excited state is being solvated preferentially.

probe molecules synergistically, while as if the solvent molecules fail to create any hydrogen bonding network, then under those conditions either of the two solvents will solvate the probe molecule preferentially and hence no synergism is being observed. This is the reason that we do not observe any synergism in the case of the alcohol–CCl₄ binary mixture, as CCl₄ tends to have zero hydrogen bond donating ability, and hence the formation of a hydrogen bonding network is absent. Once CCl₄ is replaced by CHCl₃, due to the presence of hydrogen, this molecule acts as a potential hydrogen donor for the formation of hydrogen bond with the oxygen of MeOH molecules results in the formation of MeOH–CHCl₃ clusters. Hence the MeOH–CHCl₃ binary mixture exists as a continuous network held by hydrogen bonds and the clusters of the binary mixture incline to solvate probe molecules synergistically.

In addition to hydrogen bonding network formation in the binary mixture, the dipole moment of probe molecules also plays an important role in deciding the nature of solvation. As we know, the nature of solvation around a probe molecule is decided by the structure of solvation sphere around it, when the dipole moment of probe molecules is small, as in the case of ground state of C480 and C153 (Table 1 in the Supporting Information), the structure of binary solvent mixture held intact by hydrogen

Table 1. Kamlet–Taft Parameters of Organic Solvents Used in the Measurements: HBD Ability (α), HBA Ability (β), and Polarity/Polarization (π^*)^{18,19}

solvent	α	β	π^*
methanol	98	66	60
ethanol	86	75	54
1-butanol	79	84	40
chloroform	20	10	58
carbon tetrachloride	00	10	28

bonding network, remains rigid in the solvation sphere. The intersolvent clusters are no longer perturbed, which consequently provides enough stabilization to the system with the resulting synergism as the main form of solvation. In case of *p*NA, the ground state dipole moment being comparatively large, will create enough perturbation in its immediate surroundings. These induced perturbations destabilize the binary solvent MeOH–CHCl₃ clusters in such a way that, not to permit the formation of binary solvation layer and hence instead of solvating the *p*NA synergistically, only one solvent among the two components will solvate the probe preferentially. This phenomenon is also

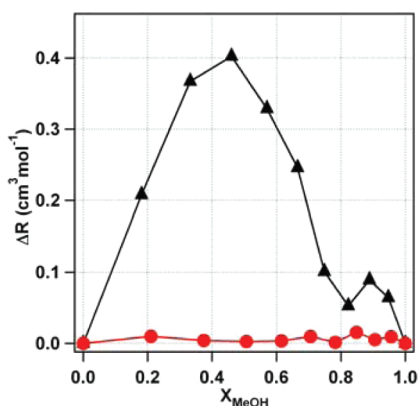


Figure 6. Molar refractivity difference between the experimental and theoretical values in MeOH + CHCl₃ (black ▲) and MeOH + CCl₄ (red ●).

supported by the absence of any synergism observed through fluorescence study for all probe molecule under consideration. The excited state dipole moment of C480 and 4-AP is larger than the ground state, which is eventually characterized by the generation of large perturbation in the excited state, and consequently, either of the solvents will preferentially solvate the excited state and thus no synergism is observed.

3.2. Molar Refractivity Measurements. Refractive index measurements were carried out in order to confirm the inter-component interactions in the binary mixture. The molar refractivity is a characteristic of the molecular structure of binary mixed solvent and is both an additive and a constitutive property. The molar refractivity (cm³ mol⁻¹) of a binary mixture is given by⁴⁷

$$R_{\text{Exp}} = \frac{(n^2 - 1)}{(n^2 + 2)} \left(\frac{X_{S1}M_{S1} + X_{S2}M_{S2}}{\rho} \right) \quad (3)$$

where n , X_{S1} , X_{S2} , M_{S1} , M_{S2} , and ρ are the refractive index of solvent mixture, mole fraction of solvent 1 and 2, molar masses of solvent 1 and 2 and the density of mixed solvents, respectively. If we consider that the two solvent components interact ideally with each other, then their molar refractivity, called as ideal molar refractivity (cm³ mol⁻¹) is given by following equation

$$R_{\text{Ideal}} = X_{S1} \left(\frac{(n_{S1}^2 - 1)}{(n_{S1}^2 + 2)} \right) \left(\frac{M_{S1}}{\rho_{S1}} \right) + X_{S2} \left(\frac{(n_{S2}^2 - 1)}{(n_{S2}^2 + 2)} \right) \left(\frac{M_{S2}}{\rho_{S2}} \right) \quad (4)$$

where the symbols have their usual meaning. The difference between the experimentally obtained molar refractivity values and ideal refractivity will give us the magnitude of interactions between the two solvent components:

$$\Delta R = R_{\text{Exp}} - R_{\text{Ideal}} \quad (5)$$

Since molar refractivity is a direct measure of electron polarization induced by the influence of constituent solvent molecules on each other in the binary mixture, so as the value of ΔR exceeds 0.1, it will direct us toward the molecular interactions shared by solvent molecules with respect to each other. Figure 6 shows the variation of ΔR against the mole fraction of MeOH for MeOH–CHCl₃ binary mixture with maximum deviation being observed at ca. $X_{\text{MeOH}} = 0.45$. This comprehends that the

electronic clouds of the constituent binary molecules interact to the maximum extent at ~ 0.45 mol fraction of MeOH in the MeOH–CHCl₃ binary mixture. Similar behavior is as well observed for other binary mixtures viz; EtOH–CHCl₃ and *n*-BuOH–CHCl₃ (see Supporting Information). These varied electronic polarizations generated by the differential proportions of the components of binary mixtures interact with the solute molecules to a varied extent and hence result in shift of the absorption maxima as shown in Figure 2b. However, such kind of behavior was not experienced by the dye molecules in MeOH–CCl₄ binary mixture, where preferential solvation of the dye molecule by MeOH is observed in the binary mixture. Thus, molar refractivity measurements act as a deterministic tool to probe the interaction of solvent binary mixtures with the solute molecules, especially in terms of the nature of solvation. These refractive index measurements augment the proposition of the existence of synergism between the binary solvent clusters and the probe molecules. From refractivity data, as mentioned earlier the maximum interactions between the solvent components in the binary mixture occurs at ca. $X_{\text{MeOH}} = 0.45$ and from absorption measurements the maximum deviation is also observed at the same mole fraction and hence supports the involvement of synergistic nature of solvation.

3.3. Proton-NMR Study of MeOH–CHCl₃ Binary Solvent Mixture. To furnish a deeper and more relevant understanding about the microscopic structure of binary solvent mixture, proton-nuclear magnetic resonance (¹H NMR) measurements were carried out. As observed in the absorption spectroscopic and molar refractivity measurements, there is definitely a kind of interaction prevailing between molecules of different solvents which is distinct than the intrasolvent interactions leading to the deviation of molar refractivity from ideality. In MeOH–CHCl₃ binary mixture, the solvent molecules interact through the formation of hydrogen bonding network and hence as the proportion of either of the components is changed, the local electronic cloud around the hydrogen bonded hydrogen atoms of each solvent changes and was directly observed as a change in the chemical shift. This change in chemical shift of proton of MeOH and CHCl₃ in the binary mixture provides a direct evidence of MeOH–CHCl₃ network formation. The nature of network between MeOH and CHCl₃ molecules is explained by proposing the following models.

3.3.1. Model for Chloroform Proton in MeOH–CHCl₃ Binary Mixture. The observed chemical shift (δ_{obs}) of CHCl₃ proton in binary mixture was found to shift toward the upfield region with increase in proportion of CHCl₃ as shown in Figure 7a and the individual NMR spectra is shown in the Supporting Information. In pure chloroform, the CHCl₃ molecules exist as self-aggregate.⁴⁸ It is presumed that the increasing the proportion of MeOH in the binary mixture results in the loss of self-association of CHCl₃ molecules and leads to the formation of H-bond between CHCl₃ and MeOH. In MeOH–CHCl₃ binary mixture, the observed chemical shift of CHCl₃ proton is taken as a linear combination of chemical shift of self-associated chloroform molecules (δ^{CC}) and chemical shift of CHCl₃ proton hydrogen-bonded to MeOH (δ^{CM}) and can be written as

$$\delta_{\text{obs}} = \frac{X_{\text{CC}}^{\text{b}}}{X_{\text{C}}} \delta^{\text{CC}} + \frac{X_{\text{CM}}^{\text{b}}}{X_{\text{C}}} \delta^{\text{CM}} \quad (6)$$

where X_{CC}^{b} , X_{CM}^{b} , and X_{C} are the mole fraction of CHCl₃ in the self-aggregate form, mole fraction of chloroform bonded to

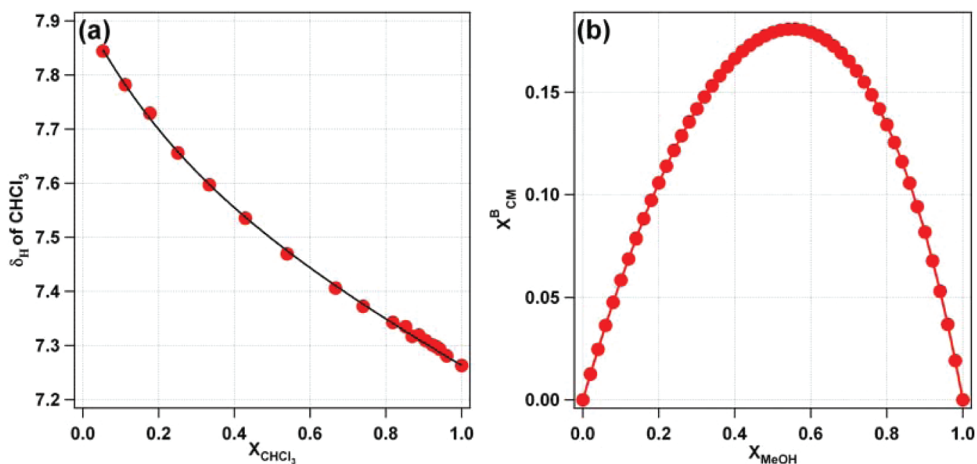


Figure 7. ^1H NMR data of CHCl_3 in $\text{MeOH}-\text{CHCl}_3$ binary mixture (a) Chemical shift of CHCl_3 proton in different proportion of CHCl_3 and (b) plot between mole fraction of CHCl_3 bonded to MeOH vs mole fraction of MeOH . The black line in graph a is the best fitted line.

MeOH and total mole fraction of CHCl_3 in the mixture (i.e., $X_C = X_{CC}^b + X_{CM}^b$) respectively. At very high proportion of CHCl_3 , i.e. when, $X_C \rightarrow 1$

$$\lim_{X_C \rightarrow 1} \delta_{\text{obs}} \equiv \delta^{\text{CC}} \quad (7)$$

At infinity small CHCl_3 proportion ($X_C \rightarrow 0$), CHCl_3 molecules solely interact with the surrounding MeOH molecules through the hydrogen bonding network in the binary mixture. In this regime, the observed chemical shift of CHCl_3 proton is thus equal to that of CHCl_3 bonded to MeOH molecules.

$$\lim_{X_C \rightarrow 0} \delta_{\text{obs}} \equiv \delta^{\text{CM}} \quad (8)$$

Experimentally observed chemical shift of pure chloroform will be same as that in self-aggregate form (δ^{CC}). However, unlike δ^{CC} we cannot directly obtain δ^{CM} . The value of δ^{CM} is thus determined by fitting the NMR data. Equation 6 can be rewritten as

$$\delta_{\text{obs}} = \delta^{\text{CM}} + \frac{X_{CC}^b}{X_C} (\delta^{\text{CC}} - \delta^{\text{CM}}) \quad (9)$$

Substituting X_{CC}^b/X_C by a normalized fitting function as shown below

$$\frac{X_{CC}^b}{X_C} = \frac{(-a_1 \exp(-b_1 X_C) - a_2 \exp(-b_2 X_C) + a_1 + a_2)}{(-a_1 \exp(-b_1) - a_2 \exp(-b_2) + a_1 + a_2)} \quad (10)$$

The NMR data set corresponding to the chemical shift of chloroform proton in the $\text{MeOH}-\text{CHCl}_3$ binary mixture was fitted to obtain the unknown parameters a_1 , a_2 , b_1 , b_2 , and δ^{CM} . The fitting of NMR data of CHCl_3 proton shown in Figure 7a. Substituting the magnitude of fitting parameters and the value of X_C in eq 10, we obtained the fraction of chloroform bonded to chloroform in the binary mixture of particular composition. Consecutively, the fraction of chloroform bonded to methanol has been calculated from the following equation

$$X_{CM}^b = X_C - X_{CC}^b \quad (11)$$

The calculated value of fraction of chloroform bonded to methanol is plotted against MeOH mole fraction as shown in

Figure 7b. The maximum value is found to be 0.56 mol fraction of MeOH .

3.3.2. Model for Methanol –OH Proton in a $\text{MeOH}-\text{CHCl}_3$ Binary Mixture. In the same set of binary mixture, not only is there a shift in the chemical shift position of CHCl_3 proton but also the position of MeOH proton is also getting affected. It is found that the observed chemical shift (δ_{obs}) of MeOH proton in binary solvent mixture is shifted toward the downfield region with increasing MeOH mole fraction (for NMR spectra, see Supporting Information). Increasing the proportion of CHCl_3 causes the self-aggregation of MeOH molecules to minimize and the interactions with the added CHCl_3 molecules to initiate, resulting in the shielding of MeOH proton. The theory to describe this model is based on the same model proposed earlier for CHCl_3 proton and the terms have their usual meanings. The main equation relating the observed NMR chemical shift values with the chemical shift values of $\text{MeOH}-\text{MeOH}$ self-aggregated and $\text{MeOH}-\text{CHCl}_3$ interactions is

$$\delta_{\text{obs}} = \frac{X_{MM}^b}{X_M} \delta^{\text{MM}} + \frac{X_{MC}^b}{X_M} \delta^{\text{MC}} \quad (12)$$

where X_{MM}^b , X_{MC}^b , and X_M are the mole fraction of MeOH in the self-aggregate form, mole fraction of MeOH bonded to CHCl_3 , and total mole fraction of MeOH in the mixture (i.e., $X_M = X_{MM}^b + X_{MC}^b$) respectively.

The equation used for fitting the chemical shift data of MeOH proton is the same as eq 10, and the final equation with which the NMR data set corresponding to MeOH proton is fitted, is given by

$$\delta_{\text{obs}} = \delta^{\text{MC}} + \frac{X_{MM}^b}{X_M} (\delta^{\text{MM}} - \delta^{\text{MC}}) \quad (13)$$

The fitting of the NMR data by the above-mentioned equation is shown in Figure 8a. Using the equation $X_{MC}^b = X_M - X_{MM}^b$, by substituting the value of X_{MM}^b corresponding to every mole fraction of MeOH , the mole fraction of MeOH at which strongest interaction between MeOH and CHCl_3 molecules exist is furnished as shown in Figure 8b. The maximum in the plot representing the strong hydrogen bonding between CHCl_3 and MeOH molecules corresponds to 0.26 mol fraction of MeOH .

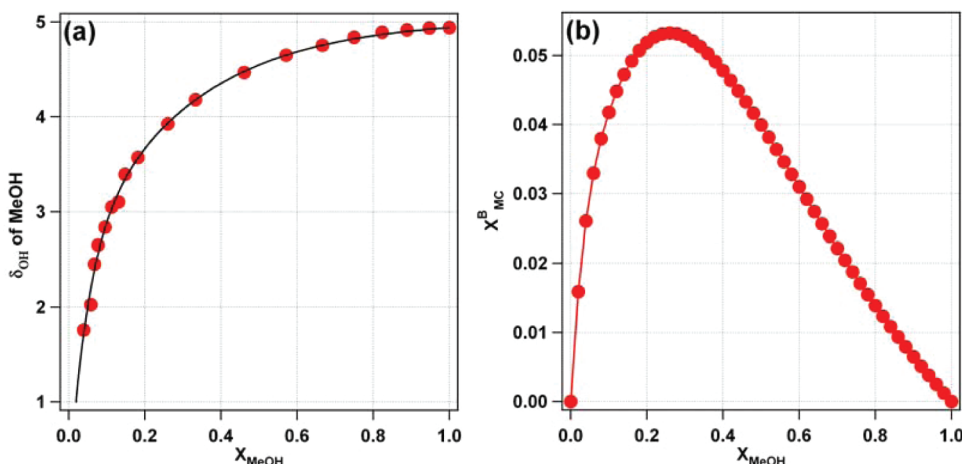


Figure 8. ^1H NMR data of MeOH in MeOH–CHCl₃ binary mixture (a) Chemical shift of MeOH hydroxy proton in different proportion of MeOH (b) plot between mole fraction MeOH bonded to CHCl₃ vs mole fraction of MeOH. The black line in graph a is the best fitted line.

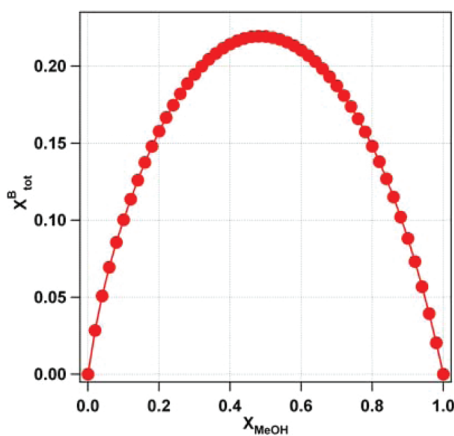


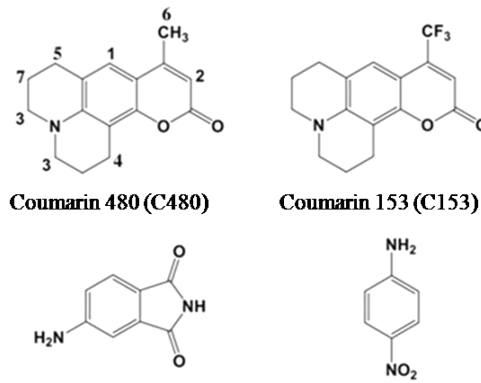
Figure 9. Plot showing total hydrogen bonding interaction of MeOH–CHCl₃ mixture ($X_{\text{tot}}^{\text{b}}$) as a function of mole fraction of MeOH in MeOH–CHCl₃ binary mixture.

Proton NMR analysis suggests that the fraction of MeOH hydrogen bonded to CHCl₃ is different from fraction of CHCl₃ bonded to MeOH at a particular mole fraction of MeOH in the mixture. The difference in the maximum position of both X_{MC}^{b} and X_{CM}^{b} is interpreted in terms of relative aggregation of MeOH with CHCl₃ and CHCl₃ with MeOH and it turns out to be an extended hydrogen bond network is being present between MeOH and CHCl₃ with a ratio of MeOH:CHCl₃ = 1:2.15. On the basis of the above analysis, it is proposed that in a binary mixture of MeOH–CHCl₃, one MeOH molecule is associated with ca. two CHCl₃ molecules through hydrogen bonding and one CHCl₃ molecule is hydrogen bonded to one MeOH molecule. The total interaction may be simply calculated by summing X_{MC}^{b} and X_{CM}^{b} as

$$X_{\text{tot}}^{\text{b}} = X_{\text{MC}}^{\text{b}} + X_{\text{CM}}^{\text{b}} \quad (14)$$

A plot of $X_{\text{tot}}^{\text{b}}$ as a function of x_{MeOH} will eventually determine the mole fraction of MeOH corresponding to strongest hydrogen bond networking in the MeOH–CHCl₃ binary mixture, and the value is found to be 0.48 (as shown in Figure 9), which is the approximately the same value obtained from refractivity measurements [$X_{\text{MeOH}}(\Delta R^{\text{Max}}) = 0.45$], and from the UV-vis

Scheme 1. Structure of Probe Molecules Used in the Steady State Absorption and Emission Measurements^a



Coumarin 480 (C480) Coumarin 153 (C153)
4-Aminophthalimide (4-AP) p-nitroaniline (pNA)

^a The atom numbers given in coumarin 480 correspond to the labels for the protons whose chemical shift values are given in the Supporting Information.

absorption study of a solvatochromic dye [$X_{\text{MeOH}}(\Delta E_T^{\text{Min}}) = 0.46$]. Thus, we propound that the addition of MeOH to CHCl₃ introduces microscopic heterogeneity in the resulting binary solvent mixture.

The ^1H NMR data was also measured for C480 in the MeOH–CHCl₃ binary mixture. The data reveals that there is a change in the chemical shift position of proton number 3 and 6 (Scheme 1a) compared to the chemical shift position in the individual bulk solvents, although the change is very small (see Supporting Information). The smaller change in chemical shift is ascribed to the small dipole moment in the ground state of C480. The NMR data of C480 in MeOH, CHCl₃ and in the 0.46 mol fraction of MeOH in MeOH–CHCl₃ binary mixture is shown in Table 2 in the Supporting Information. It suggests that, the binary mixture behaves like a different entity compared to its bulk counterparts and interacts with the probe molecule in a different fashion than the way bulk solvents do. This enunciates the existence of specific/nonspecific probe molecule-solvent pair interactions.

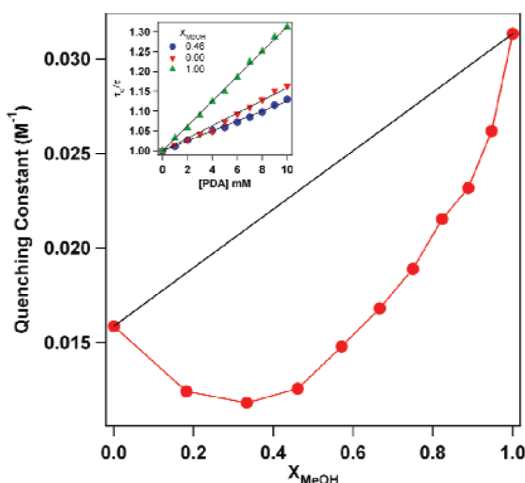


Figure 10. Plot showing variation of fluorescence quenching constant (K_q) with respect to the mole fraction of MeOH in MeOH–CHCl₃ binary mixture. Inset in the graph shows Stern–Volmer plot of C480 in bulk MeOH, bulk CHCl₃, and 0.46 mol fraction of MeOH in MeOH–CHCl₃ binary mixture.

3.4. Fluorescence Quenching in Binary Solvent Mixture. The presence of quencher can affect the lifetime of fluorophore molecules either through static interactions or through dynamic pathways.⁴⁹ Static quenching is a consequence of complexation between fluorophore and quencher molecules, while as dynamic quenching is limited by the diffusion of quencher molecules and thus being a function of solvent property like hydrogen bonding. To know quantitatively the extent of interactions prevailing in a binary solvent mixture of MeOH and CHCl₃, the fluorescence quenching study of C480 by 1,2-phenylenediamine (PDA) was done. The dynamic nature of quenching was experimentally observed by measuring the effect of quencher on the lifetime of C480, whose concentration was kept at 5 μ M and the concentration of PDA was varied from 0 to 10 mM (see Supporting Information). The observed rate of quenching as a function of mole fraction of MeOH in MeOH–CHCl₃ binary mixture were plotted as shown in Figure 10. In pure CHCl₃ the observed value of quenching rate constant is found to be 1.5879 M⁻¹. As the proportion of MeOH in the MeOH–CHCl₃ binary mixture increases, the rate constant of quenching first decreased until $X_{\text{MeOH}} = 0.46$, where the deviation from ideality is observed to be maximum (see Supporting Information, Figure S8) and then increased. In pure MeOH the value of quenching rate constant is found to be 3.1333 M⁻¹. As mentioned above, the rate of dynamic quenching is affected by the interaction of quencher with the solvent molecules. In other words, the greater the extent of interaction between molecules of binary mixture, the greater restriction they will impose on the movement of quencher toward the fluorophore and hence will retard the rate of quenching. The large deviation in quenching constant observed for 0.46 mol fraction of MeOH–CHCl₃ binary mixture inferences the maximum restriction posed on the diffusion of quencher molecules toward the fluorophore and thus comprehends the existence of stronger hydrogen bonding between MeOH and CHCl₃ molecules corresponding to this mole fraction. This observation supports the existence of stronger MeOH–CHCl₃ intermolecular interactions observed through UV–vis spectroscopy, NMR and refractivity measurements.

3.5. Solvent Exchange Model for MeOH–CHCl₃ Solvent Mixture. A modified Bosch solvent exchange model has been developed to correlate the transition energy (E_T) of solvatochromatic indicator (i.e., in our case C480) in MeOH–CHCl₃ solvent mixture.¹³ Essentially, such model consider the formation of solvent cluster in the cybotactic zone. The modified model differs from the original Bosch and Cornnors model in terms of the solvent composition in the binary solvent complex. In the present model, we have taken a 1:2 stoichiometry ratio for MeOH and CHCl₃ as evident from the ¹H NMR and other spectroscopic measurement. The formation of the mixed solvent structure was assumed to follow a two step process as $M + C \rightleftharpoons MC$ with equilibrium constant $K_1 = X_{MC}/X_M X_C$ and $MC + C \rightleftharpoons MC_2$ with equilibrium constant $K_2 = X_{MC_2}/(X_M - X_{MC_2})(X_C - X_{MC_2})$, where X_{MC_2} , X_{MC} , X_M and X_C are mole fraction of the solvent aggregate, intermediate species, MeOH and CHCl₃ respectively. These are related to the mole fractions of the mixed solvent (X_M^0 , X_C^0) as

$$X_C^0 = X_C + \frac{2}{3} X_{MC_2} \quad (15)$$

$$X_M^0 = X_M + \frac{1}{3} X_{MC_2} \quad (16)$$

$$\begin{aligned} X_M^0 + X_C^0 &= X_M + X_C + X_{MC_2} \\ &= X_M^s + X_C^s + X_{MC_2}^s = 1 \end{aligned} \quad (17)$$

Herein, the term X_{MC} exclude from equation, because it is considered as intermediate product and unstable. This quantity has taken under assumption such as

$$X_{MC} = a X_M^0 X_C^0 \quad (18)$$

where a is a constant. The mole fraction of solvent aggregate X_{MC_2} can be written as

$$X_{MC_2} = \frac{3}{10K_2} a - \frac{3}{10K_2} \sqrt{a^2 - \frac{20}{3} a (K_2)^2 X_M^0 (1 - X_M^0)^2} \quad (19)$$

where

$$a = 1 + K_2 - X_M^0 K_2 + \frac{5}{3} a X_M^0 K_2 (1 - X_M^0) \quad (20)$$

The E_T value of the mixed solvent system is written as

$$E_T = \frac{X_C^s E_{TC} + X_M^s E_{TM} + X_{MC_2}^s E_{TMC_2}}{X_C^s + X_M^s + X_{MC_2}^s} \quad (21)$$

where $X_{MC_2}^s$, X_M^s , and X_C^s are mole fraction of the solvent aggregate, MeOH, and CHCl₃ in the solvation sphere of the probe molecule, respectively, and E_{TC} , E_{TM} , and E_{TMC_2} are the transition energies of solvatochromic probe molecule in pure CHCl₃, MeOH, and MeOH–CHCl₃ solvent aggregate.

There are two possible solvent exchange processes in the solvation sphere, defined as



The equilibrium constants of the above process can be written as

$$f_{M/C} = \frac{X_M^s/X_C^s}{X_M/X_C} \quad (24)$$

and

$$f_{MC_2/C} = \frac{X_{MC_2}^s/X_C^s}{X_{MC_2}/X_C} \quad (25)$$

where, all terms are of their usual meaning. This is to note that $f_{M/C}$ is a measure of the probe to be more preferentially solvated by MeOH solvent to CHCl_3 , while $f_{MC_2/C}$ quantified the efficacy of the indicator to be synergistically solvated by solvent aggregate rather than the pure solvent counterparts. In this case, E_T of mixed solvent system can be expressed as

$$E_T = E_{TC} + \frac{X_M^0 \beta + \delta \left[\frac{3}{10K_2} \alpha - \frac{3}{10K_2} \sqrt{\alpha^2 - \frac{20}{3} \alpha (K_2)^2 X_M^0 (1 - X_M^0)^2} \right]}{1 - X_M^0 + f_{M/C} X_M^0 + \gamma \left[\frac{3}{10K_2} \alpha - \frac{3}{10K_2} \sqrt{\alpha^2 - \frac{20}{3} \alpha (K_2)^2 X_M^0 (1 - X_M^0)^2} \right]} \quad (26)$$

where,

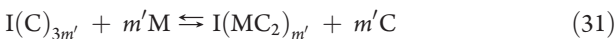
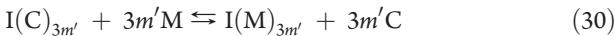
$$\beta = (E_{TM} - E_{TC})f_{M/C} \quad (27)$$

$$\delta = (E_{TMC_2} - E_{TC})f_{MC_2/C} - \frac{1}{3}(E_{TM} - E_{TC})f_{M/C} \quad (28)$$

$$\gamma = f_{MC_2/C} - \frac{1}{3}(f_{M/C} + 2) \quad (29)$$

Equation 25 has been taken under limitation by the choice of equilibrium constant K_2 . The sensitivity of E_T is guided by MeOH, CHCl_3 , and mixed solvent structure in the microsphere solvation shell, not by bulk. Therefore, a direct estimation of K_2 from the E_T values of mixture solvent system is risky. The estimation of both parameters (K_2 and $f_{MC_2/C}$) at same instant is very difficult and may lead to a huge error in results.

If we consider formation of MC_2 solvent structure on the microsphere of solvation shell, the m model (i.e., $m = 3m'$) of solvent exchange processes are given as



For this process, the equilibrium constants ($f_{M/C}$ and $f_{MC_2/C}$) are defined by

$$f_{M/C} = \frac{X_M^s/X_C^s}{(X_M/X_C)^{3m'}} \quad (32)$$

And

$$f_{MC_2/C} = \frac{X_{MC_2}^s/X_C^s}{(X_{MC_2}/X_C)^{m'}} \quad (33)$$

Finally, the value of E_T in microsphere of solvation shell of MeOH– CHCl_3 solvent aggregate can be expressed as

$$E_T = E_{TC} + \frac{\beta(X_M^0)^{3m'} + (E_{TMC_2} - E_{TC})f_{MC_2/C}(X_M^0)^{m'}(1 - X_M^0)^{2m'}}{(1 - X_M^0)^{3m'} + f_{M/C}(X_M^0)^{3m'} + f_{MC_2/C}(X_M^0)^{m'}(1 - X_M^0)^{2m'}} \quad (34)$$

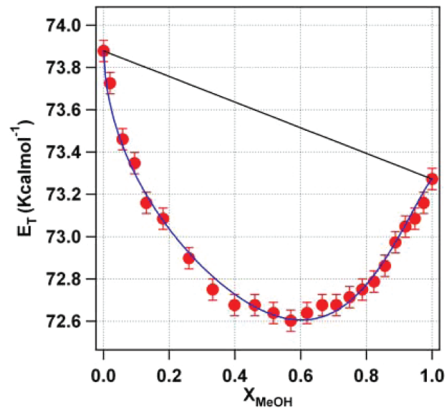


Figure 11. Plot of molar transition energy of C480 plotted as a function of MeOH mole fraction in MeOH– CHCl_3 binary mixture. The solid line is the fitting following eq 34.

The present hypothetical model gave a good idea for the synergistic mixtures where values of E_T of mixture (E_{TMC_2}) are found to be lower than E_T values of pure solvent. The variation of E_T of C480 as a function of mole fraction of methanol has been fitted with eq 34 and is shown in Figure 11. The m model gives a more appropriate fitting to the experimental result and also a reasonable explanation of the MeOH– CHCl_3 binary solvent mixture properties. The m value suggests the number of solvent molecules in microsphere of solvation shell of the probe molecule affecting its transition energy. In the present case the value of m is found to be 1.8 (ca. 2). The formation of solvent aggregates in the solvation sphere induces large deviation in polarity (i.e., $E_{TMC_2} = 71.9$) compare to bulk counterparts ($E_{TM} = 73.3$ and $E_{TC} = 73.9$). In the fitting, the value of $f_{MC_2/C}$ is found to be 1.061 where as $f_{M/C}$ is 0.454 clearly indicate the synergistic behavior of solvation. The result attributes that the strong H-bonding network between hydrogen donor and hydrogen acceptor solvent guided more polar environment in binary solvent system.

4. CONCLUSION

UV-vis absorption spectroscopy using solvatochromic probe molecules, molar refractivity and proton-NMR measurements were pursued to explore the structure and solvation behavior of binary solvent mixture. A strong synergistic solvation was observed for the mixtures of hydrogen bond donating (e.g., chloroform) and accepting solvent (e.g., alcohols like methanol, ethanol, n-butanol) pairs, which causes solvatochromic probe molecules to sense increased polarity compared to the bulk counterparts. Such strong synergism was not observed when chloroform was replaced by carbon tetrachloride. The origin of the strong synergism was explained in terms of solvent–solvent interactions as evidenced from probe dependence, molar refractivity, proton NMR measurements, and solvent exchange model. The solvation behavior of MeOH– CHCl_3 binary mixture shows strong probe dependence with no synergism observed when p-nitroaniline was taken as the solvatochromic probe, which is ascribed to the higher ground state dipole moment of p-nitroaniline (8.8 D) relative to C480 (6.3 D). Surprisingly, the synergistic signature is no longer observed for C480 in MeOH– CHCl_3 binary mixture employing fluorescence measurements, which is substantiated by higher excited state dipole moment of C480 (13.1 D). Such strongly

perturbed systems (due to high dipole moment) do not allow persistence of hydrogen bonding network, resulting in preferential solvation instead of synergism. The analysis of proton-NMR data corresponding to chloroform and methanol protons suggest the structure of binary solvent mixture through the existence of about two hydrogen bonds per methanol molecule and single hydrogen bond for each chloroform molecule. Diffusion controlled dynamic quenching of C480 fluorescence by 1,2-phenylenediamine in the binary solvent mixture also suggested the presence of strong H-bonding network.

■ ASSOCIATED CONTENT

Supporting Information. Plots of absorption maxima vs volume fraction and mole fraction, plot showing the difference between ideal and experimental molar electronic transition energy, molar refractivity difference between the experimental and theoretical values, proton NMR spectra, difference of the experimental value of quenching constant and the ideal value, and Stern–Volmer plots and tables of ground and excited state dipole moments, chemical shifts of C480 protons, and magnitudes of quenching constants. This material is available free of charge via the Internet at <http://pubs.acs.org>.

■ AUTHOR INFORMATION

Corresponding Author

*E-mail: psen@iitk.ac.in. Fax: +91-512-259-7436.

■ ACKNOWLEDGMENT

S.G. and S.R. thank the CSIR (Counsel of Scientific and Industrial Research—India) for awarding fellowships. This work is financially supported by the Board of Research in Nuclear Sciences (BRNS), Department of Atomic Energy (DAE), Government of India. 4-AP is a generous gift from K. Bhattacharyya, IACS, Kolkata, India.

■ REFERENCES

- (1) Bhattacharyya, K. *Chem Commun.* **2008**, 25, 2848.
- (2) Basu, S.; Vutukuri, D. R.; Thaymanavan, S. *J. Am. Chem. Soc.* **2005**, 127, 16794.
- (3) (a) Sando, G. M.; Dahl, K.; Owrusky, J. C. *J. Phys. Chem. B* **2007**, 111, 4901. (b) Shannigrahi, M.; Pramanik, R.; Bagchi, S. *Spectrochim. Acta A: Mol. Biomol. Spectrosc.* **2003**, 59, 2921.
- (4) Dixit, S.; Crain, J.; Poon, W. C. K.; Finney, J. L.; Soper, A. K. *Nature* **2002**, 416, 829.
- (5) Gazi, H. A. R.; Biswas, R. *J. Phys. Chem. A* **2011**, 115, 2445.
- (6) Catalan, J.; Diaz, C.; Garcia-Blanco, F. *J. Org. Chem.* **2000**, 65, 9226.
- (7) Mukherjee, S.; Sahu, K.; Roy, D.; Mondal, S. K.; Bhattacharyya, K. *Chem. Phys. Lett.* **2004**, 128, 133.
- (8) Banerjee, D.; Laha, A. K.; Bagchi, S. *J. Photochem. Photobiol. A: Chem.* **1995**, 85, 153.
- (9) Ray, N.; Bagchi, S. *J. Phys. Chem. A* **2005**, 109, 142.
- (10) Maitra, A.; Bagchi, S. *J. Phys. Chem. B* **2008**, 112, 2056.
- (11) Ramakrishnan, V.; Sarua, A.; Kuball, M.; Abdullah, A. F. *J. Raman Spectrosc.* **2009**, 40, 921.
- (12) Silva, P. L.; Bastos, E. L.; Secoud, A. E. *J. Phys. Chem. B* **2007**, 111, 6173.
- (13) (a) Roses, M.; Rafols, C.; Ortega, J.; Bosch, E. *J. Chem. Soc. Perkin Trans. 2* **1995**, 1607. (b) Skwierczynski, R.; Connors, K. *J. Chem. Soc. Perkin Trans. 2* **1994**, 467. (c) Bosch, E.; Roses, M.; Herodes, K.; Leito, I.; Koppel, I.; Taal, V. *J. Phys. Org. Chem.* **1996**, 9, 403. (d) Ortega, J.; Rafols, C.; Bosch, E.; Roses, M. *J. Chem. Soc. Perkin Trans. 2* **1996**, 1497.
- (14) Maitra, A.; Bagchi, S. *J. Mol. Liq.* **2008**, 137, 131.
- (15) Gayathri, B. R.; Mannekutla, J. R.; Inamdar, S. R. *J. Mol. Struct.* **2008**, 889, 383.
- (16) Salari, H.; Khodadabi-Moghaddam, M.; Hariffl-Mood, A. R.; Gholami, M. R. *J. Phys. Chem. B* **2010**, 114, 9586.
- (17) Laha, A. K.; Das, P. K.; Bagchi, S. *J. Phys. Chem. A* **2002**, 106, 3230.
- (18) Kamlet, M. J.; Taft, R. W. *J. Am. Chem. Soc.* **1976**, 98, 377.
- (19) Kamlet, M. J.; Abboud, J. L. M.; Abraham, M. H.; Taft, R. W. *J. Org. Chem.* **1983**, 48, 2877.
- (20) Mancini, P. M. E.; Terenzani, A.; Adam, C.; Vottero, L. R. *J. Phys. Org. Chem.* **1999**, 12, 430.
- (21) Marcus, Y. *J. Chem. Soc., Perkin Trans. 2* **1994**, 1015.
- (22) Bevilacqua, T.; Goncalves, T. F.; Venturini, C. G.; Machado, V. G. *Spectrochim. Acta A: Mol. Biomol. Spectrosc.* **2006**, 65, 535.
- (23) Mancini, P. M. E.; Terenzani, A.; Adam, C.; Perez, A. C.; Vottero, L. R. *J. Phys. Org. Chem.* **1999**, 12, 207.
- (24) Mancini, P. M. E.; Terenzani, A.; Adam, C.; Vottero, L. R. *J. Phys. Org. Chem.* **1997**, 10, 849.
- (25) Perez, A. C.; Mancini, P. M. *J. Phys. Org. Chem.* **2009**, 22, 197.
- (26) Schneider, H. In *Solute-Solvent Interactions*; Coetzee, J. F., Ritchie, C. D., Eds.; Dekker: New York, 1969; Vol. 1, p 301.
- (27) Dohnal, V.; Tkadlecova, M. *J. Phys. Chem. B* **2002**, 106, 12307.
- (28) Klingens, J.; Palmas, P. *Phys. Chem. Chem. Phys.* **2011**, 13, 10661.
- (29) Tkadlecova, M.; Havlicek, J.; Dohnal, V. *Can. J. Chem.* **1995**, 73, 1406.
- (30) Tkadlecova, M.; Dohnal, V.; Costas, M. *Phys. Chem. Chem. Phys.* **1999**, 1, 1479.
- (31) Yadava, S. S.; Yadav, N. *Can. J. Chem. Eng.* **2011**, 89, 576.
- (32) Iglesias, M.; Orge, B.; Tojo, J. *J. J. Chem. Eng. Data* **1996**, 41, 218.
- (33) Dawber, J. G.; Etemad, S. *J. Chem. Soc. Faraday Trans.* **1990**, 86, 3725.
- (34) Singh, P. P.; Sharma, B. R.; Sidhu, K. S. *Can. J. Chem.* **1979**, 57, 387.
- (35) Bauer, M.; Rollberg, A.; Barth, A.; Spange, S. *Eur. J. Org. Chem.* **2008**, 4475.
- (36) Mancini, P. M. E.; Terenzani, A.; Adam, C.; Perez, A. C.; Vottero, L. R. *J. Phys. Org. Chem.* **1999**, 12, 713.
- (37) Seth, D.; Sarkar, S.; Pramanik, R.; Ghatak, C.; Setua, P.; Sarkar, N. *J. Phys. Chem. B* **2009**, 113, 6826.
- (38) Banerjee, S.; Roy, S.; Bagchi, B. *J. Phys. Chem. B* **2010**, 114, 12875.
- (39) Dhumal, N. R. *Spectrochim. Acta A* **2011**, 79, 654.
- (40) Bae, S. Y.; Arnold, B. R. *J. Phys. Org. Chem.* **2004**, 17, 187.
- (41) Gratias, R.; Kessler, H. *J. Phys. Chem. B* **1998**, 102, 2027.
- (42) Durov, V. A.; Tereshin, O. G.; Shilov, I. Y. *J. Mol. Liq.* **2005**, 121, 127.
- (43) Prabhakar, S.; Weingartner, H. *Z. Phys. Chem. Neue Folge* **1983**, 137, 1.
- (44) Bhattacharyya, I.; Kumar, P.; Goswami, D. *J. Phys. Chem. B* **2011**, 115, 262.
- (45) Reichardt, C. *Chem. Rev.* **1994**, 94, 2319.
- (46) Reichardt, C. *Chem. Soc. Rev.* **1992**, 21, 147.
- (47) Glasstone, S. *Textbook of Physical Chemistry*; Interscience: New York, 1946.
- (48) Jumper, C. F.; Emerson, M. T.; Howard, B. B. *B. B. J. Chem. Phys.* **1961**, 35, 1911.
- (49) Lakowicz, J. R. *Principles of Fluorescence Spectroscopy*, 3rd ed.; Springer: Berlin, 2006; Chapter 8.